CHAPTER 1

INTRODUCTION

1.1 Introduction to ferrite

Ferrites (Fig. 1.1) have fascinated great interest for many years due to their broad application areas. The term "ferrite" is frequently utilized to designate a class of magnetic oxide-based compounds that comprises iron oxide as a principal constituent. They belong to the group of magnetic nanoparticles, having a high degree of structural stability. Ferrites are ferrimagnetic oxide-based ceramics that demonstrate magnetically conducting and electrically non-conducting behavior. Magnetite (Fe_3O_4), also entitled loadstone, is a naturally occurring ferrite and is considered the first magnetic material identified by the ancient people [(Srivastava and Yadav, 2012)].

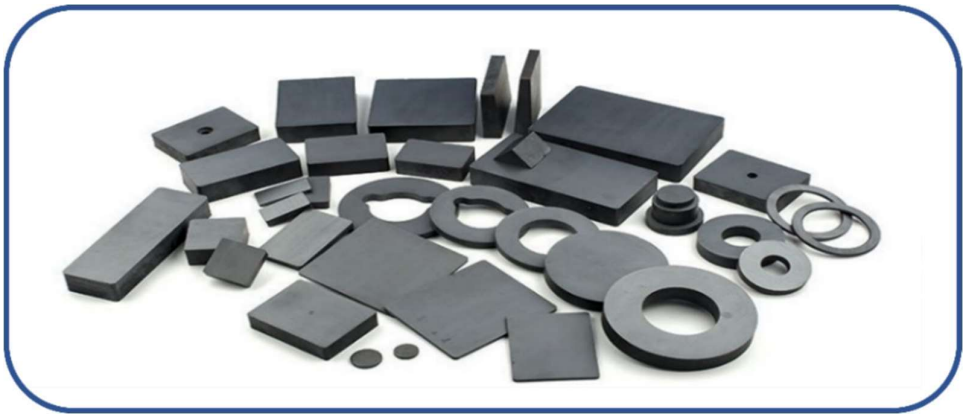

Figure 1.1 Ferrite magnets in different shapes and sizes [(Corp., 2018)].

The story of ferrite begins in 1949 while searching for a suitable ferromagnetic material capable of providing a very high resistivity value to minimize the eddy current losses. Continuous development in current electronic technology carries up an enormous demand for high-frequency range operating devices that require a magnetic material with excellent electromagnetic properties. The broad area of ferrite application continues to nurture due to the lessening of material dimension into the nanoscale. The successful commercial application of ferrites was initiated after 1950 in television, radio, computer circuits, and devices working at high frequency.

A market survey report generated by an EMR corporation suggests that the development and application of ferrite materials are accomplished by a huge volume of ferrite production, approximately 1.24 million tons in 2020 (shown in Fig. 1.2). It is driven by the progress of automobiles and other feasible advanced applications. Assisted by the growing demands and newer technical advancements of ferrite materials, the market growth is expected (upward at a compound annual growth rate of 3.0%.) to achieve further evolution in the estimated period of 2022-2027. It will likely attain a huge production of 1.44 million metric tons by the end of 2026 [(EMR Corporation, 2020)]. The increasing market demand and continuously growing technical advancements provide a driving force to focus on the research with ferrite materials.

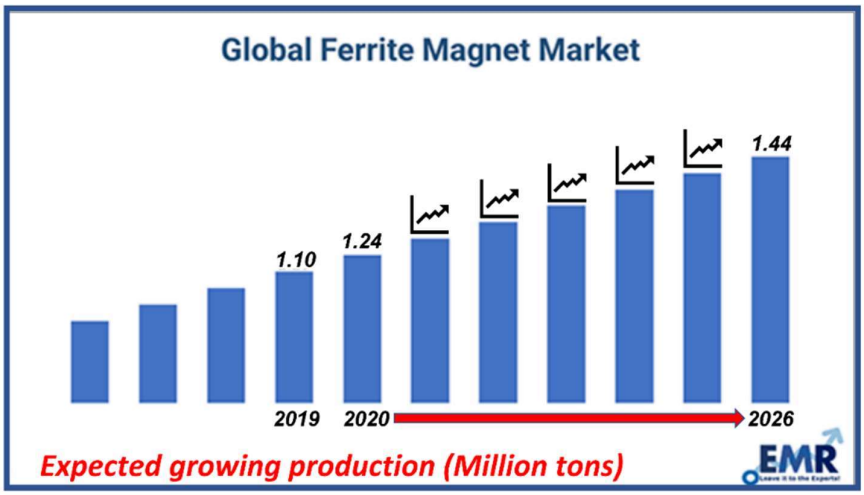

Figure 1.2 Globally forecasted growing market trends for the development of ferrite materials [(EMR Corporation, 2020)].

1.2 Classification of ferrite

Ferrites are classified into two groups based on magnetic coercivity: a) soft ferrite and b) hard ferrite. Based on the crystal structure (atomic arrangements), ferrites can be classified into four categories: spinel ferrite, garnet, orthoferrite, and hexaferrite.

1.2.1 Classification based on the magnetic coercivity

1.2.1.1 Soft ferrite

Soft ferrites are considered by low coercivity value (H_c), high saturation magnetization (M_s), and tiny magnetic remanence after magnetization (shown in Fig. 1.3 (a)). These ferrites can be easily magnetized and demagnetized. Soft ferrites can accumulate or transfer magnetic energy in alternating waveforms (sine, square, pulse, etc.). It can not be applied at high frequencies due to high eddy current losses within it. Hence, soft ferrites became the most desirable material to be used in making cores of switch-based power supplies, inductors, and radio-frequency transformers [(Ravinder, 1992)]. The zinc ferrite ($ZnFe_2O_4$), lithium ferrite ($Li_{0.5}Fe_{2.5}O_4$), manganese ferrite ($MnFe_2O_4$), copper ferrite ($CuFe_2O_4$), and nickel ferrite ($NiFe_2O_4$), are considered as soft ferrite materials.

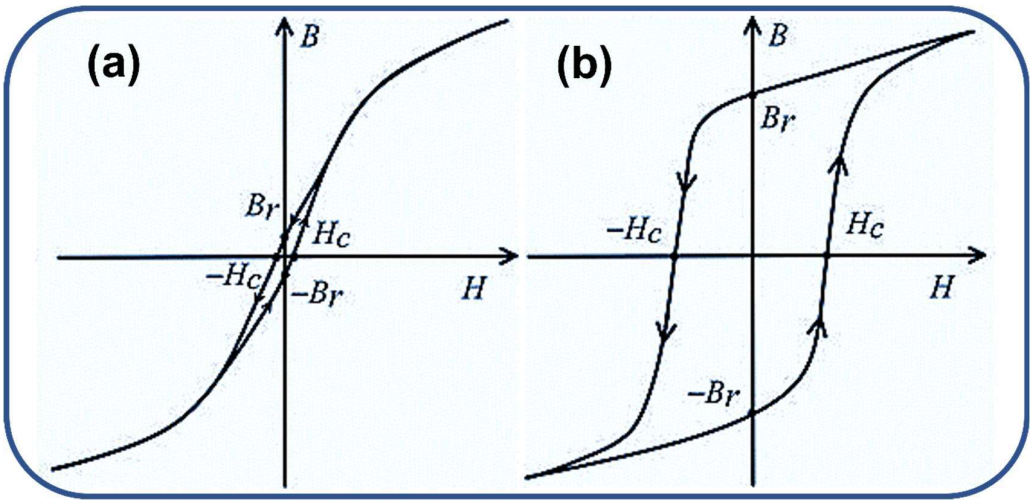

Figure 1.3 Hysteresis loop representation of (a) soft ferrite and (b) hard ferrite [(Chang, 2020)].

1.2.1.2 Hard ferrite

Hard ferrites are categorized by the high value of coercivity (nearly 2000 Oe or more) and high magnetic retentivity after magnetization (shown in Fig. 1.3 (b)). These hard ferrites are utilized as a permanent magnet, including numerous applications like

refrigerators, medical tools, motors, loudspeakers, computer devices, and automotive systems. The strontium hexaferrite ($SrFe_{12}O_{19}$) and barium hexaferrite ($BaFe_{12}O_{19}$) are hard ferrite materials [(Singh *et al.*, 2008)].

1.2.2 Classification based on the crystal structure

1.2.2.1 Spinel ferrite

Spinel ferrites can be attributed to their general chemical formula MFe_2O_4, where M is a divalent metal ion. The crystal structure of these ferries is FCC (face-centered cubic) with eight formula units per unit cell (shown in Fig. 1.4). On behalf of the cationic distribution within the tetrahedral and octahedral interstitial sites, spinel ferrites can further be classified into three types: (a) spinel ferrite in which all divalent and trivalent metal cations occupies the tetrahedral and octahedral interstitial positions, termed as normal spinel ferrite, (b) if half of the trivalent metal cations occupy the tetrahedral sites, termed as inverse spinel ferrite, (c) if the metal cations occupy the intermediate distribution between normal and inverse type arrangement, termed as random spinel ferrite [(Shaikh *et al.*, 2020), (Valenzuela, 2012)].

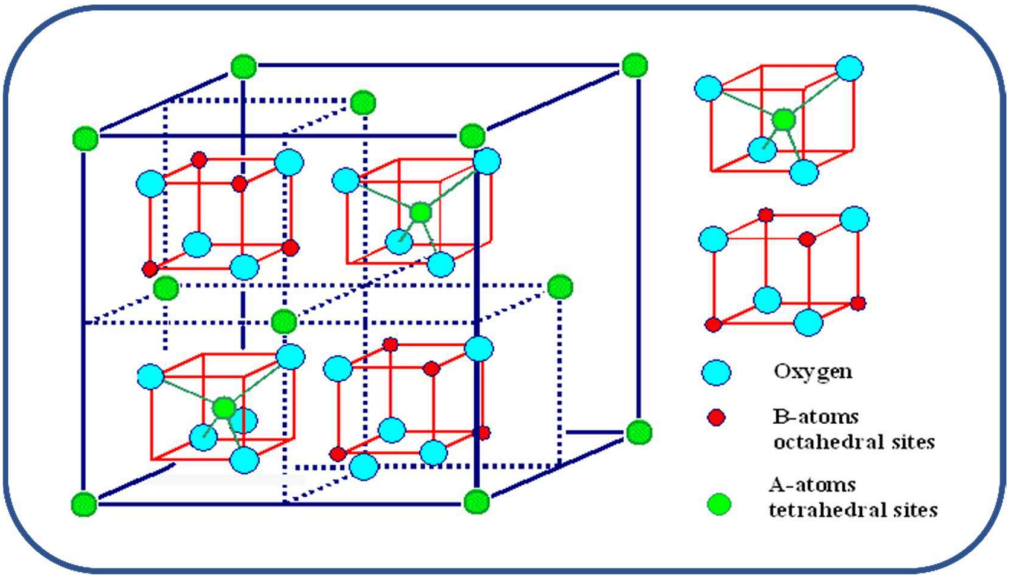

Figure 1.4 Crystal structure representation of normal spinel ferrite [(Issa *et al.*, 2013)].

1.2.2.2 Garnet

Garnet ferrites can be ascribed by the chemical formula $R_3Fe_5O_{12}$, where R is a trivalent rare-earth ion like Dy, Sm, Gd & Y. Its unit cell is cubic that comprises eight formula units within each unit cell. The metal cations are distributed over three different sites; tetrahedral voids (A-site), octahedral voids (B-site), and dodecahedral voids (C-site). Rare-earth ions get surrounded by eight oxygen ions and occupy C-site. Iron ions are distributed among A and B sites in a ratio of 3:2. The crystal structure of yttrium iron garnet (YIG) having a general formula of $Y_3Fe_5O_{12}$ is shown in Fig. 1.5. These are unique magnetic ceramics with optical transparency and are used in magneto-optical applications [(Shaikh *et al.*, 2020), (Zhang *et al.*, 2013), (Valenzuela, 2012)].

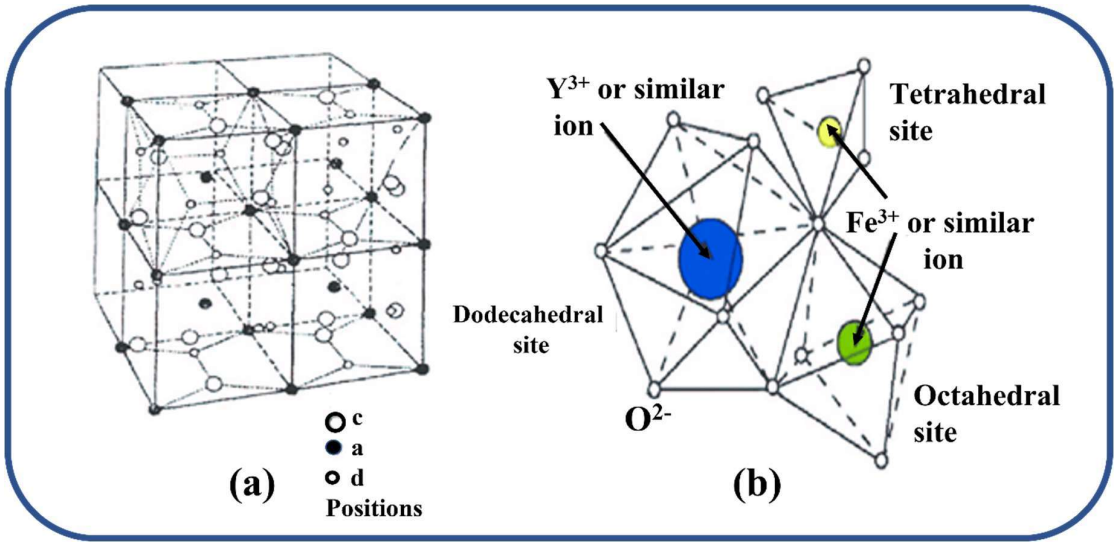

Figure 1.5 Crystal structure representation of garnet ferrite [(Zhang *et al.*, 2013)].

1.2.2.3 Ortho-ferrite

Ortho-ferrites can be recognized by a general chemical formula of $RFeO_3$, where R denotes a large trivalent rare-earth ion like Y, Ho, & Er. Orthoferrites are known by the distorted perovskite structure with orthorhombic unit cells (crystal structure of yttrium orthoferrite ($YFeO_3$) is shown in Fig. 1.6). It demonstrates weak ferromagnetism resulting

from the minor canting behavior in the alignment of two antiferromagnetically coupled lattices. These ferrites have an extremely high tendency of domain wall motion and found their applications within communication-related equipment and versatile sensors, etc.

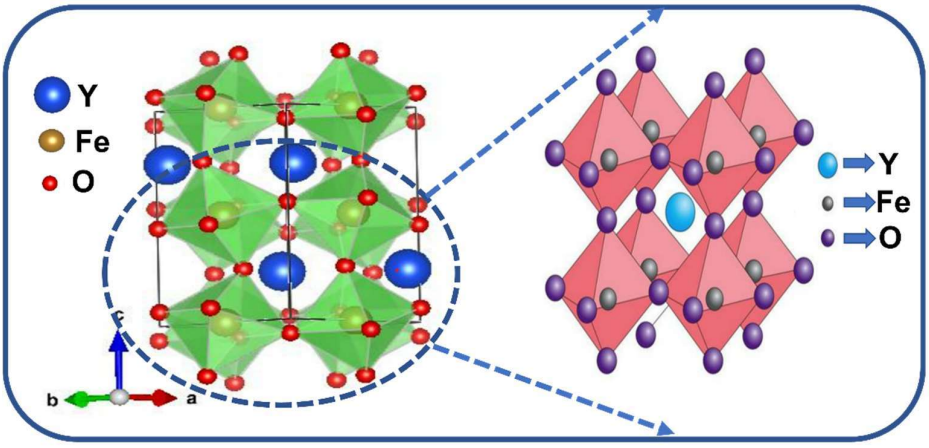

Figure 1.6 Crystal structure representation of $YFeO_3$ ortho-ferrite [(Majewska and Drushliak, 2019)].

1.2.2.4 Hexaferrite

The hexaferrite materials exhibit the magnetoplumbite kind of crystal structure, originating from the naturally occurring mineral having a similar name [(Vinnik *et al.*, 2019) (Delacotte et al., 2018)]. The hexagonal ferrite's major composition consists of a formula of $MeFe_{12}O_{19}$, where Me is a divalent cation generally referred to as Sr, Ba, or Pb. The hexaferrite materials have hexagonal symmetry, having a major axis "*c*" and a minor axis "*a*" [(Delacotte *et al.*, 2018)]. Utmost of these hexaferrite compounds shows ferrimagnetic behavior, with few antiferromagnetic in nature [(Hibst, 1982), (Kojima, 1982)].

1.3 General properties of ferrite

The properties of ferrites depend upon several factors, but it majorly depends on the elemental compositions and the process employed for the preparation. Nevertheless, the

properties of the concerned ferrite can be engineered by introducing impurity phases or other abnormalities within the crystal structure to shelter a wide range of applications. The basic properties of ferrites can be described below:

(a) posses moderate value of dielectric constant (order of thousands at lower frequencies), dropping to about 20 or 10 at higher frequencies (microwave region), due to the closely packed oxygen ions [(Prakash and Baijal, 1985)].

(b) having grayish or black color, which can be explained due to the nearly identical energies of the 4*s* & 3*d* states. It can also be correlated to visible range absorption [(Fernandes *et al.*, 2019)].

(c) act as a semiconductor underneath the stimulus of an externally applied electric field [(Khairy and Gouda, 2015)].

(d) show better hardness and brittle, governed by the closely packed oxygen ions forming ionic bonds [(Niederberger *et al.*, 2004)].

(e) best known for their magnetic properties, including magnetic anisotropy (existence of easy magnetization axis), hysteresis behavior and permeability (high for soft ferrite and low for hard ferrite), and Curie temperature (the temperature at which the magnetic moment's orientation is destroyed) [(Jalili *et al.*, 2019), (Manjurul Haque, Huq, and Hakim, 2008), (Niederberger *et al.*, 2004)].

1.4 Applications of ferrite

Ferrites can be considered the most prominent magnetic material utilized in several applications, including home appliances, communication equipment, and devices related to data processing. The important applications of ferrite materials are mentioned in Fig. 1.7. A wide range of applications, which offers technical importance within various fields for ferrites, can be attributed due to their structural, electrical, and magnetic properties

[(Kumari *et al.*, 2020), (Issa *et al.*, 2013), (Valenzuela, 2012)]. The ferrite materials are also utilized as photovoltaic sensitizers in dye-sensitized solar cell devices, making electrodes within lithium ion-based batteries, making symmetric supercapacitors (double layered), electrolytic capacitors (hybrid) & pseudocapacitors, as a catalyst for hydrogen production using the water splitting approach, as a gas & humidity sensor [(Shaikh *et al.*, 2020)].

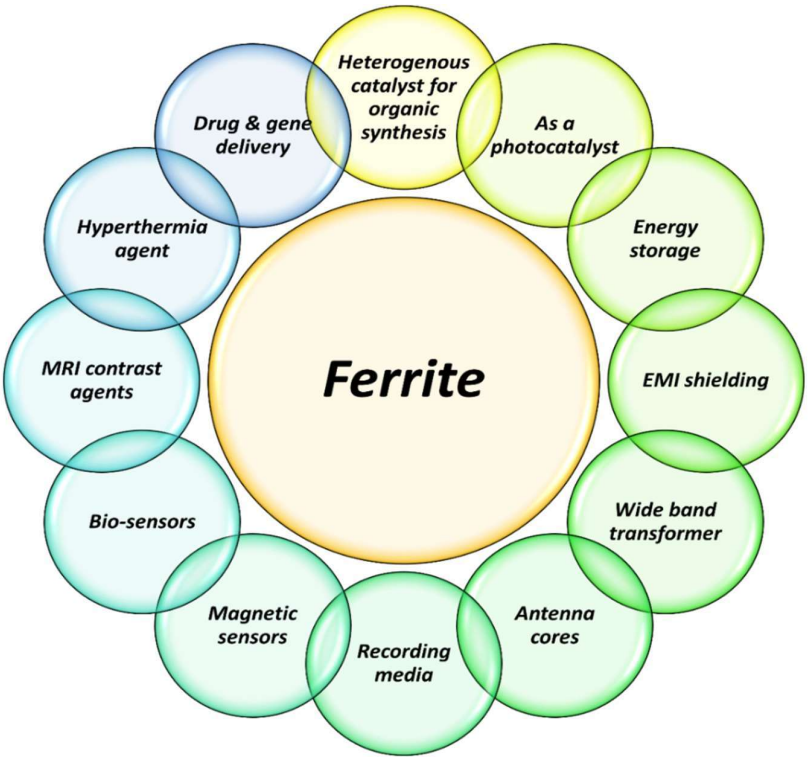

Figure 1.7 The general applications of ferrite materials.

1.5 The structure, composition, and characteristics of hexagonal ferrite

The magnetoplumbite ($PbFe_{7.5}Mn_{3.5}Al_{0.5}Ti_{0.5}O_{19}$) mineral was first introduced in 1925, and the determination of its crystal structure (revealed to be hexagonal) was performed in 1938. The term hexaferrite can be treated as a group of interrelated compounds having rhombohedral or hexagonal crystal (shown in Fig. 1.8) symmetry. The hexaferrite materials show ferrimagnetism driven by the super-exchange interactions

between electrons of metal and oxygen ions. The hexaferrite materials possess a high resistivity value due to the presence of several magnetic interactions that facilitate these materials' application at high frequencies. The elemental compositions can be described using MeO-Fe_2O_3-BaO ternary phase diagram (shown in Fig. 1.9). Here, Me signifies a divalent cation (possible choices are Co, Zn, Fe, Ni, Cu & Mg) [(Pullar, 2012), (Valenzuela, 2012)]. The phase diagram reveals that most of these hexaferrite phases are formed within a triangular portion made of $BaFe_{12}O_{19}$ (M), $Me_2Fe_4O_8$ (S) & $Ba_2Me_2Fe_{12}O_{22}$ (Y) at its edges.

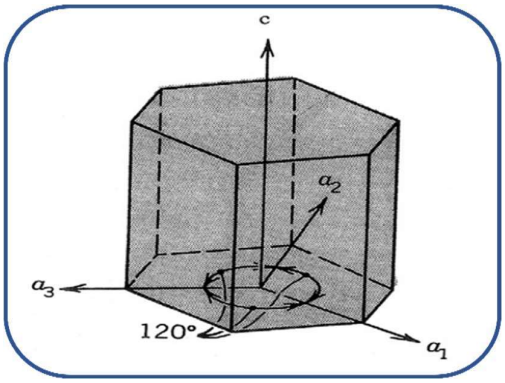

Figure 1.8 A hexagonal crystal demonstrating lattice parameters *a* and *c* [(Pullar, 2012)].

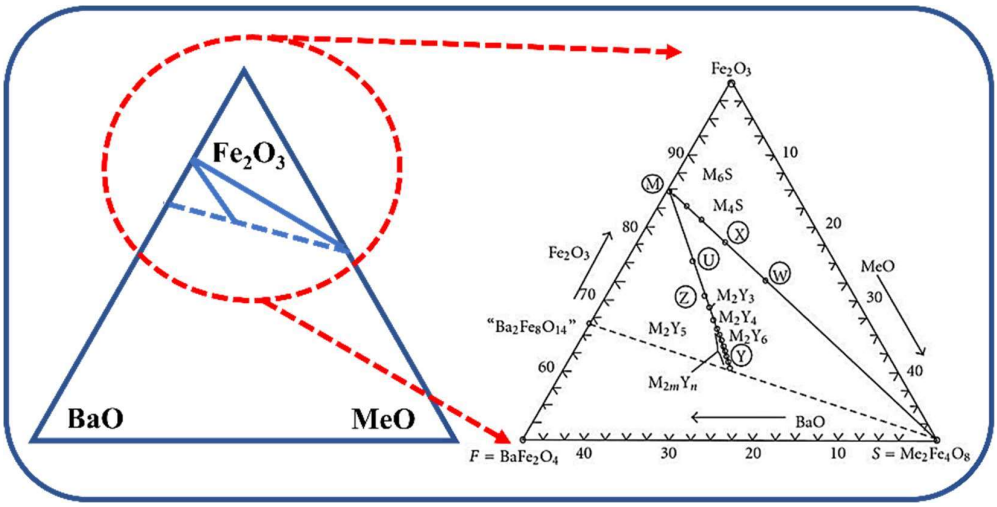

Figure 1.9 The upper section of the ternary phase diagram (Fe_2O_3-BaO-MeO) presents several hexaferrite phases [(Pullar, 2012)].

1.5.1 Types of hexagonal ferrite

Hexaferrites are categorized into six subclasses (M, U, W, X, Y, and Z type) according to the crystal structure and corresponding arrangements of S, R, and T blocks (shown in Fig. 1.10). R block represents three oxygen layers (one oxygen atom is replaced by barium in the middle layer) with the composition of MFe_6O_{11}. S block represents spinel block that consists of two oxygen layers (three metal cations amid each layer, at four octahedral & two tetrahedral sites) with composition $Me_2Fe_4O_8$ (Me = metal cation). T block represents four layers of oxygen ions (one oxygen atom is replaced by barium in both intermediate layers) with the composition $M_2Fe_8O_{14}$ [(Kamishima *et al.*, 2011)]. The adjacent layers are affected by the replacement; as a result, the top and bottom layers disappear to accommodate both the larger-sized barium ion.

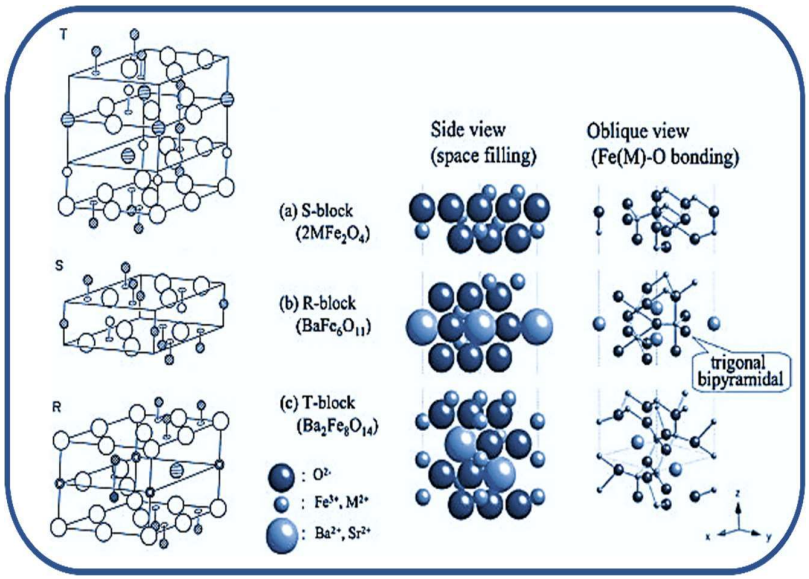

Figure 1.10 Schematic representation of basic constituting S, R, and T blocks along with side & oblique view for enhanced visualization [(Kamishima *et al.*, 2011), (Pullar, 2012)].

It also allows the conversion of trigonal bipyramidal sites (coordinated with five neighboring ions) to the tetrahedral sites (coordinated with four neighboring ions) by

ensuing a total of six octahedral & two tetrahedral sites. The categorization of these hexagonal ferrites can be understood by their stacking orders, chemical formula, and other characteristics, as tabulated in Table 1.1.

Table 1.1 Several types of cobalt-based barium hexaferrite along with their characteristics.

Hexaferrite type	Chemical formula	Molecular mass (g)	Density ρ (g/cm^{-3})	Unit cell structure	No. of oxygen layer	Magnetisation at 300 K
M	$BaFe_{12}O_{19}$	1112	5.28	RSR^*S^*	10	Uniaxial
Y	$Ba_2Co_2Fe_{12}O_{22}$	1410	5.40	3 (ST)	18	In plane
U (2M+Y)	$Ba_4Co_2Fe_{36}O_{60}$	3624	5.31	$RSR^*S^*T^*S^*$	16	In-plane
W (M+S)	$BaCo_2Fe_{16}O_{27}$	1577	5.31	$RSSR^*S^*S^*$	14	In cone
X (2M+S)	$Ba_2Co_2Fe_{28}O_{46}$	2688	5.29	3 ($RSR^*S^*S^*$)	36	In cone
Z (M+Y)	$Ba_3Co_2Fe_{24}O_{41}$	2522	5.35	$RSTSR^*S^*T^*S^*$	22	In-plane

1.5.1.1 M-type hexagonal ferrite

The generally utilized M-type hexaferrite (member of $P6_3/mmc$ space group) are $SrFe_{12}O_{19}$ (SrM) & $BaFe_{12}O_{19}$ (BaM). It possesses a hexagonal magnetoplumbite structure. It was first introduced by Phillips laboratory in the early 1950s [(Pullar, 2012)]. The M-type hexaferrite is a magnetically hard magnet with high coercivity and a high electrical resistivity of 10^8 Ω-cm. These ferrites have high uniaxial magnetocrystalline anisotropy along the *c*-axis and are cheaper to produce.

1.5.1.2 Y-type hexagonal ferrite

Y-type hexaferrite (member of the R_3m space group) was the first ferroxplana ferrites to be exposed. All Y-type ferrites possess a preferred plane of magnetization perpendicular to the *c*-axis at 300K. However, $Ba_2Co_2Fe_{12}O_{22}$ shows a cone of magnetization below -58°C and planar magnetic anisotropy above -58°C to Curie temperature [(Mahmood *et al.*, 2015), (Jotania and Virk, 2012)].

1.5.1.3 U-type hexagonal ferrite

U-type hexaferrite (member of the R_3m space group) was identified earlier as a mixed (minor) phase along with the synthesis of Y & Z-type hexaferrite. The first-ever single crystal of Zn_2U was grown successfully In 1968. All U-type ferrites show uniaxial magnetic anisotropy except $Ba_4Co_2Fe_{36}O_{60}$, which shows planar anisotropy at 300K [(Pullar, 2012)].

1.5.1.4 W-type hexagonal ferrite

The first reported single-phase W-type ferrite (member of the $P6_3/mmc$ space group) was $BaFe_2Fe_{16}O_{27}$, which has an easy magnetization axis along the hexagonal *c*-axis structure. However, it has high electrical conductivity than M-type due to the existence of Fe^{2+} ions. All the W-type ferrites have uniaxial anisotropy excepting only $BaCo_2Fe_{16}O_{27}$, having an easy cone of magnetization at a 70° angle [(Mørch *et al.*, 2019), (Pullar, 2012)].

1.5.1.5 X-type hexagonal ferrite

The first reported X-type ferrite (member of the R_3m space group) was $Ba_2Fe_2Fe_{28}O_{46}$ having an easy magnetization axis along the *c*-axis of the hexagonal structure. All the X-type ferrites have uniaxial anisotropy except $Ba_2Co_2Fe_{28}O_{46}$, which has a cone of easy magnetization at a 74° angle to the *c*-axis [(Pullar, 2012)].

1.5.1.6 Z-type hexagonal ferrite

The Z-type hexaferrite (member of the $P6_3/mmc$ space group) was discovered along with Y-type ferroxplana. All Z-type ferrites show uniaxial anisotropy parallel to the *c*-axis, whereas $Ba_3Co_2Fe_{24}O_{41}$ shows planer but complex magnetic anisotropy at 300K with at least four different anisotropic states. A single unit of Z-type hexaferrite comprises a combination of Y (ST blocks) & M (SR blocks) type hexaferrite, showing a mirror plane behavior inside the R block, repeating after every 11 oxygen layers for the next [(Pullar, 2012)].

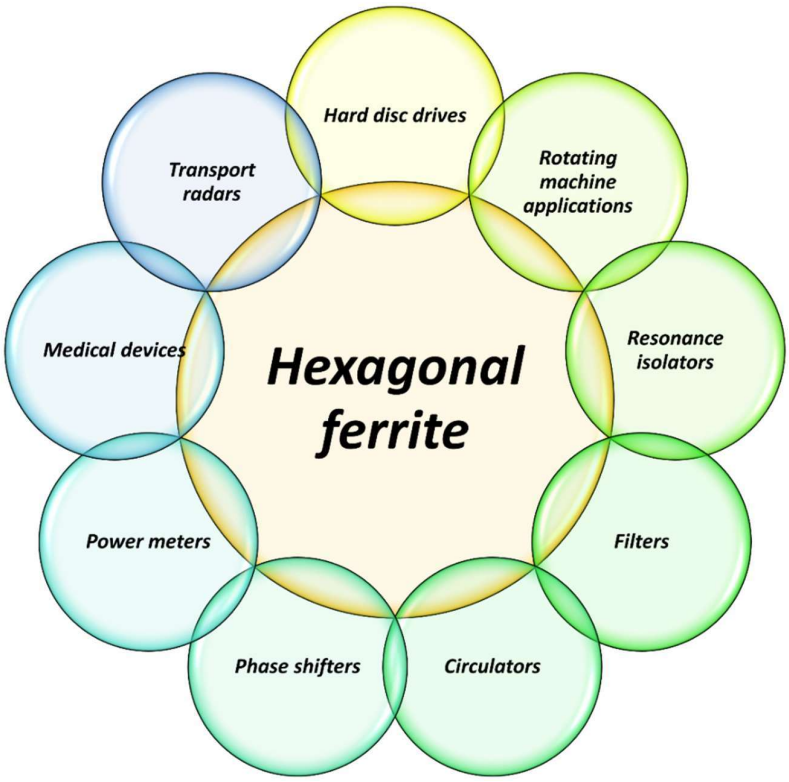

Figure 1.11 The general applications of hexagonal ferrite materials.

1.5.2 Applications of hexagonal ferrite materials

Hexaferrites are utilized in a wide range of applications, especially for rotating components within motors, sensors & actuators, power generators, varying transformers, information storage devices, antenna components for mobile communications, automobile

sectors, defense & aerospace-related equipment, biomedical devices, etc. Among all categories of ferrite materials, the most used are hexaferrite; a few of these applications are enlisted below in Fig. 1.11.

Table 1.2 Room temperature magnetic characteristics of Y-type hexaferrites [(Daigle *et al.*, 2010), (Mahmood *et al.*, 2015)].

Hexaferrite	M_s (emu/g)	H_c (Oe)	Tc (K)
Co_2-Y	27.8	106.3	613.15
Ni_2-Y	25.5	205	659.75
Zn_2-Y	42	-	403.15
Mn_2-Y	31	-	563.15
Mg_2-Y	22	100	550.15

1.6 The structure, composition, and characteristics of Y-type hexagonal ferrite

The Y-type barium hexaferrite (Me_2-Y) is the first room-temperature ferroxplana material having an easy plane of magnetization arranged perpendicular to the larger *c*-axis [(Jonker, Wijn and Braun, 1956)]. The Y-type barium hexaferrite can be described with a general formula of $Ba_2Me_2Fe_{12}O_{22}$, where Me represents a small divalent cation (the popular choices are Co, Ni, Zn, Mn, Mg, Cu, etc.) [(Mahmood *et al.*, 2015)]. The present research work focuses on the feasibility of accepting cobalt-based Y-type barium hexaferrite (Co_2-Y) within several fields of applications. However, Y-type barium hexaferrite (Me_2Y) is the most abundantly studied hexaferrite system. The resulting properties can be modified by the selection of appropriate Me ions ($Ba_2Me_2Fe_{12}O_{22}$). The influence of varying Me ions on the Y-type barium hexaferrite is illustrated in Table 1.2. The coercivity values of the samples can not be explained by their dependency on the Me ions because it is also majorly influenced by particle size. The limited research work within

the field of Y-type barium hexaferrite doesn't allow the proper justification for the variations within the magnetic properties.

1.6.1 Cobalt-based Y-type hexagonal ferrite (Co_2-Y)

The single Y-type barium hexaferrite (Co_2-Y) unit cell (member of *R3m* space group) is composed of three formula units, comprising an ordered stacking of S (consisting of two layers of hexagonal close-packed oxygen, having a general formula of $Co_2Fe_4O_8$) and T (consists of four layers of hexagonal close-packed oxygen with one Ba^{2+} ion substituting an oxygen ion in each of the two middle layers, having a general formula of $Ba_2Fe_8O_{14}$) structural blocks in the sequential order of STS*T*S**T**, where * represent a rotation of 120° about the *c*-axis [(ALBANESE, 1977), (Mahmood *et al.*, 2015)].

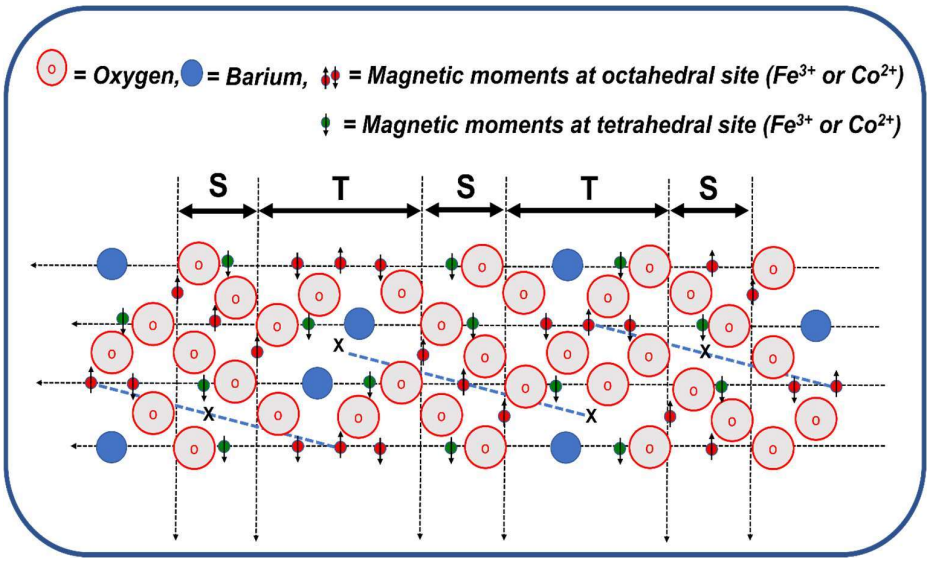

Figure 1.12 Cross-sectional view of the $Ba_2Co_2Fe_{12}O_{22}$ structure where horizontal lines are threefold symmetry axes & the arrows indicates the magnetic moment's orientation of the cations (Fe^{3+} or Co^{2+}) relative to the *c*-axis [(Pullar, 2012), (Chandel *et al.*, 2020)].

The Co_2-Y hexaferrite shows magnetic properties equivalent to the soft magnetic material with in-plane magnetic anisotropy [(Pullar, 2012), (Sudakar, Subbanna, and Kutty,

2003)]. The Co^{2+} and Fe^{3+}ions may occupy a total of six possible interstitial sites, including four octahedral sites [$3a_{VI}$ (one ion having up spin magnetism, lie within S block), $3b_{VI}$ (one ion having up spin magnetism, lie within T block), $6c_{VI}$ (two ions having low spin magnetism, lie within T block), $18h_{VI}$ (six ions having up spin magnetism, sheared within S & T block)) and two tetrahedral sites [$6c_{IV}$ (two ions having low spin magnetism, lie within S block), $6c_{IV^*}$ (two ions having low spin magnetism, lie within T block)] [(Jotania and Virk, 2012), (Mahmood *et al.*, 2015)].

The magnetization within the Y-type barium hexaferrite can be explained as a combination of separate contributions of both S and T building blocks. The single S block comprises four octahedral and two tetrahedral sites for cations. The alignment of their magnetic moments (shown within Fig. 1.12) is as follows:

S block = (4↑) octahedral and (2↓) tetrahedral = (2↑)

The single T block comprises a total of six octahedral (two moments are aligned within the tetrahedral direction) and two tetrahedral magnetic moments, resulting in a net-zero magnetic moment.

T block = (4↑ 2↓) octahedral + (2↓) tetrahedral = 0

The total vectorial sum of magnetic moments contribution from S and T blocks, which provide the overall magnetization for Co_2-Y hexaferrite, can be described as follows:

Magnetization of Co_2-Y = (8↑ 2↓) octahedral + (4↓) tetrahedral = (2↑)

This opposing magnetic spin within the T block is responsible for lower saturation magnetization values in Y-type hexaferrites as equated to other hexaferrites [(Chandel *et al.*, 2020)].

1.6.2 Synthesis & properties of Y-type barium hexagonal ferrite (Co_2-Y)

Till the date, the Y-type hexaferrites are reported to be synthesized using limited number of processes likewise solid state ceramic route [(Vinaykumar, Jyoti and Bera, 2018), (Wang *et al.*, 2012), (Fu *et al.*, 2019), (Mahmood *et al.*, 2015), (Baik, Shim and Kim, 2022), (Bierlich and Töpfer, 2012), (Kim, Rhee and Kim, 2012), (Salunkhe and Kulkarni, 2004)], sol gel [(Chand Pramanik *et al.*, 2006), (Kamba *et al.*, 2010), (Iqbal and Barkat-ul-Ain, 2009)], sol-gel autocombustion [(Rashad *et al.*, 2018), (Nadeem *et al.*, 2022), (Alrebdi *et al.*, 2022), (Carol T *et al.*, 2022), (UL-AIN, AHMED and HUANG, 2013), (Bai *et al.*, 2006), (Odeh *et al.*, 2016), (Alrebdi *et al.*, 2022), (Iqbal and Liaqat, 2010), (Shakeel *et al.*, 2019), (Ahmad *et al.*, 2018), (Ali, Shaheen, *et al.*, 2014), (Koutzarova *et al.*, 2012), (Warhate and Badwaik, 2020)], microwave assisted auto combustion method [(BADWAIK *et al.*, 2012)], flux method [(Wu *et al.*, 2022), coprecipitation method[(Jotania and Virk, 2012), (Chen *et al.*, 2011), (Nikzad *et al.*, 2015), (Lehlooh *et al.*, 2020), (Rashad *et al.*, 2018), (Daigle *et al.*, 2010)] & microemulsion method [(Ali, Islam, *et al.*, 2014)]. Majorly two synthesis processes (solid states ceramic method & sol-gel auto combustion method) are dominated over all these synthesis processes.

The Y-type hexagonal ferrites can be characterized generally by its structural parameters ranging between (a = 5.85 to 6.45 Å), (c= 43.15 to 44.45 Å), bulk density (2.85 to 5.20 g/cm^3), electrical parameters such as electrical resistivity (ρ = 1.01x10^5 to 4.9x10^9 ohm-cm), activation energy (E_a = 0.16 to 0.52 eV), drift mobility (μ_d = 2.5x10^{-15} to 3.3x10^{-12} cm^2.v^{-1}.s^{-1}), and magnetic properties likewise saturation magnetization (M_s = 13.44 to 77.11 emu/g), coercivity value (H_c = 23 to 1210 Oe), remanent magnetization (M_r = 1.58 to 17.51 emu/g), squareness ratio (S_R= 0.04 to 0.65), number of Bohr magneton (N_{BM} = 3.68 to 15.27 μ_B), etc [(Iqbal and Barkat-ul-Ain, 2009), (Ali, Islam, Ashiq, Khan,

et al., 2014), (Aslam *et al.*, 2014), (Ahmad *et al.*, 2018), (Ali, Islam, Ashiq, Asif Iqbal, *et al.*, 2014), (Chandel *et al.*, 2020)].

1.6.3 Explorations of Y-type hexagonal ferrite (Co_2-Y)

The limiting research within the exploration of Y-type barium hexaferrite materials allows only a few articles to focus on the real-time application of these materials. Moreover, the researchers are focused on the utilization of Y-type hexaferrites as a promising material within the field of microwave absorption.

In 2012, rod-shaped (responsible for the tuning of FMR frequency) copper-modified Y-type hexaferrite ($Ba_2Co_{1.8}Cu_{0.2}Fe_{12}O_{22}$) is studied, and the result shows its excellency by achieving 98% of microwave absorption within the X-band frequencies [(Xu *et al.*, 2012)].

In 2013, the cobalt-modified Y-type hexaferrite ($Ba_2Mg_{2-x}Co_xFe_{12}O_{22}$) is studied for its catalytic activity within the decomposition of N_2O. The rate of N_2O decomposition is found to increase with the incorporation of cobalt ions within the system. This enhanced catalytic activity can be suggested by increasing the redox behavior between Co^{2+} and Co^{3+} [(UL-AIN, AHMED, and HUANG, 2013)].

In 2015, the CuO-modified Y-type hexaferrite ($Ba_2Co_2Fe_{12}O_2$) is studied to be utilized as a terrestrial broadcasting antenna. The result shows that 0.6 wt% of CuO addition provides a permeability value of 2.7 & a low loss factor near about 0.05 (measured at 1 GHz). The antenna made of this material (3 mm x 3 mm x 30 mm) displays an outstanding average gain of –0.7 dBi at a frequency of 600 MHz along with a wider bandwidth of 160 MHz (far better than a dielectric antenna having a bandwidth of 110 MHz under a gain level of –5 dBi) [(Fujii *et al.*, 2015)].

In 2016, the nickel-modified Y-type hexaferrite ($BaSrCo_{2-x}Ni_xFe_{12}O_{22}$) is studied to be utilized as a passive microwave absorbing material & a substrate for magnetodielectric antenna (working up to 18 GHz). The results show its excellency with the enhanced value of electromagnetic properties (complex permittivity and permeability) [(Stergiou and Litsardakis, 2016)]. The aluminum-modified Y-type hexaferrite ($Ba_{1.5}Sr_{0.5}CoZnFe_{12-x}Al_xO_{22}$) is studied for its microwave absorption capability. The results suggest that the sample doesn't provide any significant absorption within the Ku-band of the frequency range (12.4 to 18 GHz) up to a sample thickness of 5 mm, whereas the material shows a remarkable performance at a large thickness of 8 mm (disadvantageous in terms of application), providing better microwave absorption at higher frequency region [(Song *et al.*, 2016)].

In 2017, the Y-type hexaferrite ($Ba_2Co_2Fe_{12}O_2$) is studied to be utilized as a substrate material for mobile communication antennas. The result shows that the material achieves 68.39% of radiation efficiency as compared to 82% without ferrite substrate, suggesting the miniaturization of the antenna components [(Chen *et al.*, 2017)].

In 2021, the Y-type hexaferrite-based flexible composite (polyvinylidene fluoride/reduced graphene oxide/$Ba_2Co_2Fe_{12}O_{22}$) is studied for its EMI shielding application. The results show the enhanced EMI shielding efficiency, achieving 20.14 dB of shielding effectiveness within a bandwidth of 8.48 GHz [(Anand and Pauline, 2021)]. The Y-type hexaferrite-based core-shell micro flowers ($Ba_2Co_2Fe_{12}O_{22}$/MnO_2/carbon nanotubes) are studied for their microwave absorption efficiency. The results show excellent performance within the X-band (8 GHz to 12 GHz), C-band (4 GHz to 8 GHz), and S-band (2 GHz to 4 GHz) frequencies [(He *et al.*, 2021)].

There is a need to explore different substitutions in Y-type hexagonal ferrite to tune the properties and make it suitable for various applications.

1.7 Theme of the work

This research work aims to explore the feasibility of replacing a substituted Co_2-Y ferrite to overcome the issues related to soft ferrite materials in various applications. The selection of cobalt-based Y-type barium hexaferrite ($Ba_2Me_2Fe_{12}O_{22}$) is due to the uppermost value of magnetocrystalline anisotropy among all possible choices for Me ions, i.e., Co, Ni, Zn & Cu [(Stergiou and Litsardakis, 2016)]. The cobalt-based Y-type barium hexaferrite ($Ba_2Co_2Fe_{12}O_{22}$) shows a similar magnetic profile with majorly utilized soft ferrite materials along with enhanced thermochemical stability [(Guin, Baruwati and Manorama, 2005), (Singh and Sangwa, 2017), (Jotania and Virk, 2012), (Tanasoiu, Miclea, and Dimitriu, 1996), (Schultz-Sikma *et al.*, 2011)]. The proposed Co_2-Y ferrite is applied to five versatile (heterogeneous catalyst for oxidation, heterogeneous catalyst for reduction, photocatalyst for degradation of methyl orange, microwave absorber for EMI shielding, biocompatible hyperthermia agent) applications and analyzed their properties, performance & influencing parameters.

1.8 Organization of the thesis

The thesis work is organized into nine chapters as follows

Chapter-I briefly introduces the ferrites, hexaferrites, and their classifications and applications. It also describes the theme and organization of the thesis.

Chapter–II provides a review of the current state of the art within the concerned area. The chapter explains the role of substitution in Co_2-Y hexaferrite along with the background information, supportive literature, and recently published investigations regarding all five areas of applications, considered as the objective of the present thesis.

Chapter–III offers a detailed description of the material processing & synthesis method employed for preparing substituted Co_2-Y hexaferrite. A brief explanation of all the characterization techniques utilized within this research work is also added in this section.

Chapter–IV explains the role of Ce^{3+} substitution at the Ba^{2+} site within Co_2-Y hexaferrite and analyzes its performance as a heterogeneous catalyst for oxidation of styrene.

Chapter–V clarifies the role of Ce^{3+} substitution at the Fe^{3+} site within Co_2-Y hexaferrite and examines its performance as a heterogeneous catalyst for reducing toxic nitro-organic pollutants.

Chapter–VI elucidates the role of Ti^{4+} substitution at the Fe^{3+} site within Co_2-Y hexaferrite and investigates its performance as a photocatalyst for the treatment of methyl orange contaminated wastewater.

Chapter–VII describes the role of La^{3+} substitution at the Ba^{2+} site & Mg^{2+} substitution at the Co^{2+} site within Co_2-Y hexaferrite and studies its performance as a microwave absorber for EMI shielding application.

Chapter–VIII enlightens the role of Cr^{3+} substitution at the Fe^{3+} site within Co_2-Y hexaferrite and evaluates its performance as a biocompatible hyperthermia agent.

Chapter–IX provides conclusive remarks and the future scope of the present work.

Finally, towards the end of the thesis, a complete list of references has been included, and at last, a concise list of publications and conferences related to the present research work has been enclosed.